ARMY RESEARCH LABORATORY

Description of Gun Muzzle Blast by Modified Ideal Scaling Models

Kevin S. Fansler

ARL-TR-1434 SEPTEMBER 1997

The findings in this report are not to be construed as an official Department of the Army position unless so designated by other authorized documents.

Citation of manufacturer's or trade names does not constitute an official endorsement or approval of the use thereof.

Destroy this report when it is no longer needed. Do not return it to the originator.

Army Research Laboratory
Aberdeen Proving Ground, MD 21005-5066

ARL-TR-1434 September 1997

Description of Gun Muzzle Blast by Modified Ideal Scaling Models

Kevin S. Fansler
Weapons & Materials Research Directorate

Abstract

Gun blast data from a large variety of weapons are scaled and presented for both the instantaneous energy release and the constant energy deposition rate models. For both ideal explosion models, similar amounts of data scatter occur for the peak overpressure but the instantaneous energy release model correlated the impulse data significantly better, particularly for the region in front of the gun. Two parameters that characterize gun blast are used in conjunction with the ideal scaling models to improve the data correlation. The gun-emptying parameter works particularly well with the instantaneous energy release model to improve data correlation. In particular, the impulse, especially in the forward direction of the gun, is correlated significantly better using the instantaneous energy release model coupled with the use of the gun-emptying parameter. The use of the Mach disk location parameter improves the correlation only marginally. A predictive model is obtained from the modified point source correlation.

ACKNOWLEDGMENTS

The author wishes to thank Dr. Mark Bundy for his comments and suggestions to improve this report.

INTENTIONALLY LEFT BLANK

TABLE OF CONTENTS

INTENTIONALLY LEFT BLANK

LIST OF FIGURES

INTENTIONALLY LEFT BLANK

LIST OF TABLES

INTENTIONALLY LEFT BLANK

DESCRIPTION OF MUZZLE BLAST BY MODIFIED IDEAL SCALING MODELS

1. INTRODUCTION

1.1 Background

Before guns are fired near personnel or fragile equipment that might be harmed, blast wave overpressure levels need to be accurately known over a large range of distances from the gun muzzle. Personnel and instruments may need to be located as close as 15 to 20 calibers away from a gun. On the other hand, designing an enclosure for reducing impulsive noise may require an estimate of the forces and impulses on its inside surfaces as far away as 100 calibers from the muzzle. Some of the quantities that can be used to assess gun blast at a field point are shown in Figure 1.

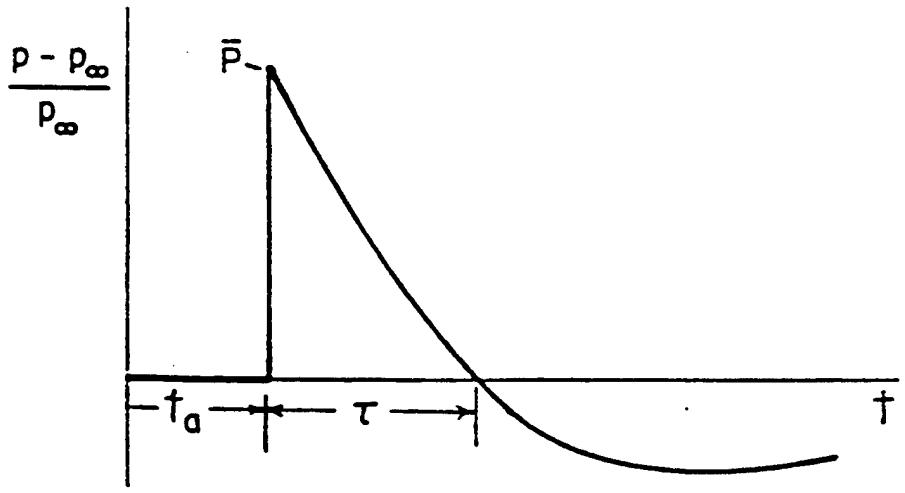

Figure 1. Schematic of Blast Wave.

This is an idealized schematic of the overpressure, nondimensionalized or scaled by the atmospheric pressure, as a function of time. Measured overpressure traces are more complicated, partly attributable to turbulent processes. Here, p is the pressure and p_∞ is the atmospheric pressure, which near sea level is approximately one bar. The scaled or nondimensionalized peak overpressure is designated as $\overline{P}$. Shown also is the time of arrival, t_a, together with the positive phase duration, τ. The impulse, I, is defined as the time integral of the positive phase for the overpressure

$$I \equiv \int_{t_a}^{t_c} \left(p - p_\infty \right) dt, \tag{1}$$

in which t_c is the time for the overpressure to become zero in the blast wave. The impulse is a very important quantity in determining if structures are reinforced adequately to withstand the blast wave. The time of arrival and positive phase duration need to be known accurately when peak overpressures and impulses at a field point result from multiple reflections of the blast wave.

The first predictions of gun blast were done using results obtained from instantaneous energy release blast from a point source. The Buckingham Pi theorem can be applied to instantaneous energy release at a point source to obtain a fundamental length, λ. The scaled peak overpressure, $\overline{P}$, becomes a function of the distance scaled by the fundamental length (Hopkinson 1915; Baker 1973). Although explosive charges will not strictly generate point source blasts, they approximate blast waves from point source blasts after a minimum scaled distance is reached (Brode 1955, 1959). Reynolds (1944) applied this point source scaling theory developed by Hopkinson (1915) to gun blast problems. Westine (1969) proposed a scaling prediction method based on high-explosive detonations in combination with the length of the gun barrel. He based his work mainly on 20-mm data that included different projectile muzzle velocities, and he developed contours for predicting peak overpressure and time of arrival for a wide range of weapons, but these contours did not extend completely around the weapons.

Smith (1974) used a different approach in his study of the blast wave produced by a 7.62-mm rifle. He combined scaled solutions to the problems of blast waves generated by a constant energy efflux with blast waves from asymmetrically initiated charges. The prediction method agreed well with the limited data.

Schmidt, Gion, and Fansler (1980) used yet another approach to predicting muzzle blast. They found that the peak overpressure correlated well with the location of the Mach disk for an equivalent steady jet whose exit conditions matched that for the pressure and the propellant gas velocity. Later, Fansler and Schmidt (1983) found that the Mach disk method of prediction was deficient in its ability to predict the peak overpressure changes with the change in the propellant temperature. However, Smith's (1974) prediction model predicted the actual trends. Fansler and Schmidt (1983) generalized and extended Smith's work (1974) to develop prediction methods for bare muzzle guns, based

on data collected in the range of 10 to 50 calibers from the gun muzzle. From dimensional analysis (Baker 1973), a scaling length, ξ, was obtained that is assumed to be proportional to the square root of the peak energy efflux from the gun muzzle. This scaling length depends on such parameters as the exit muzzle pressure, exit temperature of the propellant, and the projectile velocity at the gun muzzle. The distance from the muzzle to the field point divided by the scale length, r/ξ, yields the fundamental scaled distance. However, the blast waves are highly directional, with their peak overpressures decreasing with increasing polar angle from the forward axis direction. The form for the variation of peak overpressure with angle from the axis is obtained from asymmetrically initiated charges, or equivalently, moving charge theory (Armendt & Sperrazza 1956). This angle variation function, β, possesses one free parameter that determines how rapidly the peak overpressure falls off with increasing polar angle. The function, $\beta\ (\theta)$, is multiplied by the fundamental scale length, ξ, to obtain the modified scaled length, ξ', for gun blast. The assumed formulation for the scaled peak overpressure was

$$\overline{P} = A\left(\frac{\xi'}{r}\right)^a \tag{2}$$

in which r is the distance from the muzzle and the free parameters, A and a together with the free parameter for β, are determined by a least squares fit to peak overpressure data. The other blast wave quantities of interest were also formulated and least square fitted to data. The predicted muzzle blast quantities were implemented on a computer and can be applied for blast waves incident on surfaces to obtain the reflected pressures (Heaps, Fansler, & Schmidt 1986). Fansler (1986), noting deficiencies in the impulse model, examined additional impulse data and developed an expression that depended not only on the scaling length but also on a dimensionless parameter that depended upon the time for the gun barrel to empty. The computer-implemented technique (Heaps, Fansler, & Schmidt 1986) was updated with the improvement for treating impulse.

In the studies just cited, data were collected for distances close to the muzzle. Other people have investigated muzzle blast at greater distances. Soo Hoo and Moore (1972) primarily studied various naval guns with data taken for distances between 20 and 110 calibers but also obtained data for U.S. Army 20-mm M3 and M197 cannon. Kietzman, Fansler, and Thompson (1992) obtained overpressure data for a maximum of 400 calibers distance from a 105-mm tank cannon and noted that the angular distribution of the shock wave strength changed with distance. Pater (1981) obtained additional data and combined

his data with Soo Hoo and Moore's data. He noted that the peak sound pressure level (PSPS) decibel differences from the front of the gun to the rear of the gun decreased with distance.

Fansler, Thompson, Carnahan, and Patton (1993) obtained data from 7.62-mm rifles for a large range of distances (15 to 400 calibers) from the muzzle and for weapons shot at both high and low velocities with different lengths of barrels. The approach was similar to Fansler and Schmidt's (1983) approach but explored the use of gun blast parameters to modify the directional parameter, β. The data were fitted using several trial parameters and functions to obtain a best representative function for the peak overpressure. Time-of-arrival data were also obtained and a fit was obtained from a trial function. The impulse prediction function was obtained by assuming a positive phase duration form and expressing the impulse in terms of the peak overpressure and the positive phase duration. The positive phase duration possessed free parameters to be adjusted by a least squares fit to the impulse data.

Previous investigators developed a model assuming only one approach and often radically modified the ideal model into little semblance of the original form. This report reconsiders both the point source scaling approach and the energy efflux scaling approach as a basis for modification by the parameters that characterize gun blast. The length scale for the chosen ideal explosion is modified by parameters for the gun blast, and coefficients for these parameters are determined by least squares fitting to the data. This study assumes that functions of the gun blast parameters will be good first order corrections to the scale length for the ideal models.

2. DATA USED IN THE INVESTIGATION

Most previous scaling investigations conducted used data with less variation in key parameters (Fansler & Schmidt 1983; Smith 1974; Reynolds 1944) than are used in the current investigation. Thus, an earlier prediction model for gun blast might fit the earlier (limited) data but it might be a poor fit for other data used here. This investigation uses much of the Fansler, Thompson, Carnahan, and Patton (1993) data, but in an attempt to more accurately model the data nearer the gun, ignores the data taken at the longest distance, which was 400 calibers away from the gun muzzle. This investigation also uses some of the data of Fansler and Schmidt (1983) and Kietzman, Fansler, and Thompson (1992) to provide a greater range in gun blast parameters. In all these experiments, a gauge was positioned near the muzzle to establish a zero reference time for the

experiment. The experiment to obtain the small caliber overpressure data (7.62 mm) was conducted at ARL for distances 15 to 400 calibers from the muzzle (Fansler, Carnahan, & Patton 1993). For the current study, the data at 400 calibers will not be used. The weapons used in the test were a .300 Magnum barrel, another .300 Magnum barrel that had a reduced bore length, and a shortened carbine barrel. A schematic of the gauge positions around the gun muzzles is shown in Figure 2 for the investigation by Fansler, Thompson, Carnahan, and Patton (1993).

In addition, 105-mm tank cannon data obtained in the Kietzman, Fansler, and Thompson (1992) investigation are included. Some 30-mm weapon data from Fansler and Schmidt (1983) are also included because they can be used to extend the range of applicability to more gun systems. The propellant for the 30-mm cannon was specially selected to burn quickly in the barrel to maximize reproducibility. The propellant speed of sound at the muzzle was also experimentally found.

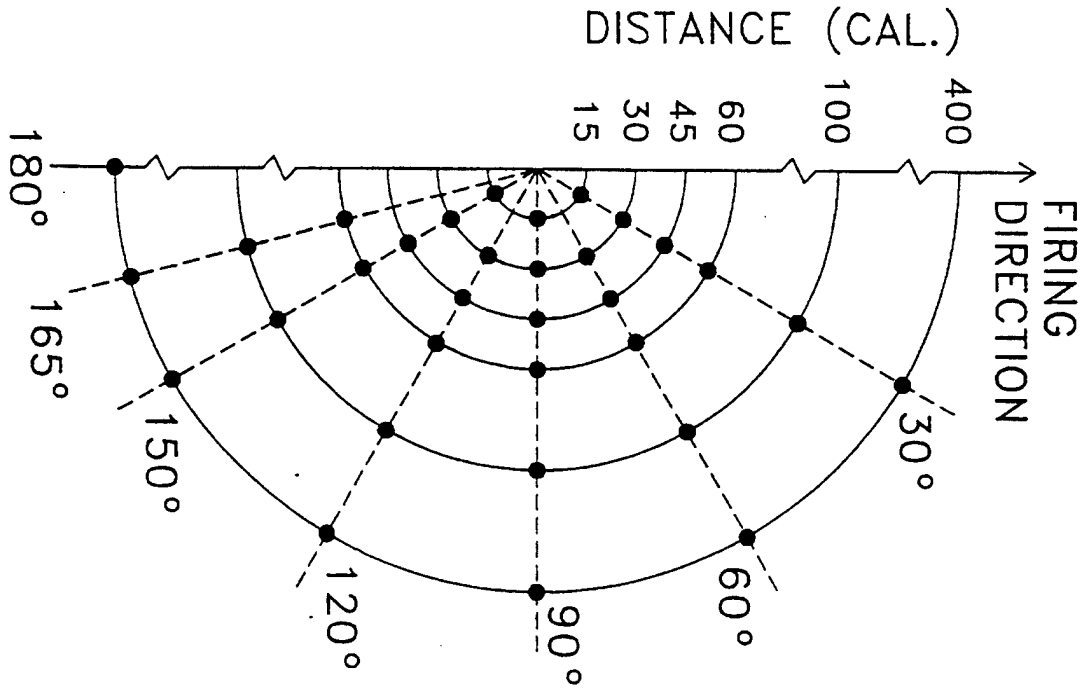

Figure 2. Gauge Positions for the Fansler, Thompson, Carnahan, and Patton Study (1993).

The loading, velocity of the projectile at the muzzle, and muzzle pressure at projectile exit are shown in Table 1 for each configuration. The muzzle pressure in the last column is the peak value immediately before the projectile exits the barrel.

Table 1. Loadings and Characteristics

Barrel	Description	Propellant Type	Charge Mass g (gr)	Projectile Velocity m/s	Muzzle Pressure MPa
.300 long Magnum	1220w70 1125w75	4831 4831	4.82 (70.0) 5.16 (75.0)	899 975	59.40 71.90
.300 short Magnum	s220w36 s125w42	4227 4227	2.48 (36.0) 2.89 (42.0)	594 792	74.90 89.60
Carbine	c13p6	2400	0.94 (13.6)	518	65.90
105 mm	105mm	M30	5966 (-)	1501	71.50
30 mm	ml0f250	M10	16.2 (250)	572	8.73

With the exception of the last two rows, the first number in the description column of Table 1 refers to the charge mass in grains, while the second number refers to the charge mass in grams. Further discussions about the firings will use these descriptions for identification. The next to the last row refers to the parameters for the 105-mm cannon shooting the M735 round (Kietzman, Fansler, & Thompson 1992).

3. SCALING APPROACHES

Because the propellant empties from the barrel in a time that depends on parameters such as gun barrel length, and the propellant exits the barrel with considerable linear momentum, no simple scaling theory (e.g., neither instantaneous nor constant energy release models) can be successfully applied to gun blast phenomena without some modifications. Nevertheless, even though the blast wave from guns is more complicated, the similarities to a particular ideal explosion may allow a related scaling technique to be used with modification by gun blast parameters to represent gun blast waves. Both instantaneous energy release explosions and constant energy efflux explosions are treatable by scaling and have been used to help describe gun blast (Reynolds 1944; Westine 1969; Fansler & Schmidt 1983, Fansler, Carnahan, & Patton 1993). For blasts generated by a constant energy efflux, *dE/dt*, the peak overpressure, $P \equiv p_p - p_\infty$ is expressed in functional terms as

$$P = P\left(r,\, p_\infty,\, a_\infty\, dE/dt\right), \tag{3}$$

in which p_p = peak value of the pressure at a given field point,

r = distance from muzzle to field point,

p_∞ = ambient density,

a_∞ = ambient speed of sound,

and dE/dt = energy deposition rate into atmosphere.

Using the Buckingham Pi theorem (Baker 1973), a scaling length for constant energy efflux explosion is obtained:

$$\xi \sim \sqrt{\left(dE/dt\right)/\left(p_\infty,\, a_\infty\right)} \tag{4}$$

and

$$\overline{P} \equiv P / p_\infty = \overline{P}\left(r/\xi\right). \tag{5}$$

Dimensional analysis shows that the time of arrival, t_a, the positive phase duration, τ, and the impulse, I, also have their scaled equivalents,

$$\bar{t}_a \equiv t_a a_\infty / \xi = \bar{t}_a\left(r/\xi\right), \tag{6}$$

$$\bar{\tau} \equiv \tau a_\infty / \xi = \bar{\tau}\left(r/\xi\right), \tag{7}$$

and

$$\bar{I} \equiv I a_\infty / \left(\xi p_\infty\right) = \bar{I}\left(r/\xi\right). \tag{8}$$

For blast waves assumed to be generated by instantaneous energy deposition at a source point, dimensional analysis leads to scaling relationships that also generate universal curves but with the energy of the explosive, E, considered a significant parameter instead of dE/dt. Similarly, as for the constant energy efflux case, it is obtained that

$$\overline{P} = \overline{P}\left(r/\lambda\right), \tag{9}$$

in which

$$\lambda = \left(\frac{E}{p_\infty}\right)^{1/3}. \tag{10}$$

The point source expressions for the scaled time, positive phase duration, and impulse are Equations (6), (7), and (8) with ξ replaced by λ.

As related before, gun blast cannot be completely characterized by either of these ideal blast models. Nevertheless, the ideal models can be modified to describe muzzle blast. The energy release rate of propellant gas from the gun muzzle exit depends upon the length of the barrel, the velocity of the projectile, and the sound speed of the propellant gas before projectile exit. As a first step in characterizing muzzle blast in terms of the constant energy efflux model, the energy deposition rate for gun blast is assumed to be the energy efflux from the muzzle exit immediately after the projectile back clears the muzzle exit. The energy deposition rate can then be written as

$$\frac{dE}{dt} = \frac{\gamma_e p_e u_e}{\gamma_e - 1}\left[1 + \frac{\left(\gamma_e - 1\right)}{2} M_e^{\,2}\right] A_e , \tag{11}$$

in which A_e is the area of the bore, M_e is the exit Mach number of the propellant flow immediately after the projectile exits the muzzle, p_e is the peak muzzle overpressure while the projectile exits the muzzle, u_e is the velocity of the propellant gas at the exit immediately after the projectile exits the muzzle, and γ_e is the specific heat ratio for the exiting propellant.

To use the instantaneous energy release model as a basis for gun blast, a value for E must be assumed. The available energy, E, is assumed to be the total energy in the propellant minus the energy expended in propelling the projectile and heating the gun tube by friction and heat transfer. The kinetic energy of the propellant gas is part of the available energy for the blast.

In addition to prescribing dE/dt and E (for use in the constant energy efflux and point source models, respectively), other dimensionless parameters are needed to modify the ideal models for accurately computing gun blast. For instance, if a gun barrel empties quickly, the peak overpressure will be higher than if the energy is released over a longer period of time. Neither the initial dE/dt nor E itself will account for this emptying time effect. Hence, an additional parameter characterizing the "blow-down" process, which can be obtained with the Buckingham Pi theorem, is used (Fansler 1986).

For the constant energy release model, the blow-down parameter is defined by the ratio of the scale for the gun tube emptying time, L/V_p (Corner 1950), to the time scale for muzzle blast, ξ / a_∞.

$$\delta_\xi \equiv \frac{La_\infty}{\xi V_p}, \tag{12}$$

in which L is the effective length of the barrel and V_p is the exit velocity of the projectile. The smaller the value of $\delta\xi$, the more quickly the barrel is emptied.

Its counterpart for the instantaneous energy release model is

$$\delta_\lambda \equiv \frac{La_\infty}{\lambda V_p} \tag{13}$$

Again, when the blow-down parameter is small, the barrel empties more quickly, which would result in the energy from the propellant being used in a more efficient manner by the gun blast wave. These expressions for the blow-down parameter are not unique, but they are simple and may be adequate representations for times to empty guns.

Another parameter that characterizes gun blast is the axial location of the Mach disc or the recompression shock that is centered on the gun bore axis (Erdos & DelGuidice 1975; Schmidt, Gion, & Fansler 1980). For the steady jet, the axial position of the Mach disc relative to the muzzle for the steady jet is given as

$$x'_M / D = M_e \sqrt{\gamma_e \bar{p}_e / 2}, \tag{14}$$

in which D is the diameter of the bore. The Mach disc location expression resembles the constant energy efflux expression but differs in the emphasis upon the Mach number for the exit flow and the exit velocity for the muzzle flow. The use of the Mach disc location as a gun parameter allows other characteristics of the gun blast flow to be expressed. It has been used with some success as a scaling factor (Schmidt, Gion, & Fansler 1980). The scale lengths for the ideal types of explosions, the blow-down parameters, and the Mach disc locations are given in Table 2 for various gun test data presented in this report.

Table 2. Blast Parameters for the Point Source and Energy Efflux Models

Designation	λ/D	$\delta\lambda$	ξ/D	$\delta\xi$	x_M/D
c13p6	39.8	0.437	9.44	1.84	15.80
s220w36	51.4	0.712	9.45	3.87	17.60
s125w42	55.6	0.462	10.40	2.47	22.30
1220w70	60.1	0.694	8.41	4.96	25.60
1125w75	63.8	0.598	9.80	3.89	26.60
105 mm	54.9	0.214	14.01	0.82	38.90
m10f250	22.2	0.955	3.08	6.88	6.58

4. RESULTS

A computer program was developed to extract the peak overpressure, the impulse (numerically calculated time integral of the positive phase for the overpressure), and the time of arrival from the obtained overpressure waveforms. Then, both the scaled peak overpressure data and the scaled impulse data are scaled with the fundamental length for each model and presented for the polar angles of 30°, 90°, and 150°. If the two models are comparable in their correlations, then modification of the scale length with the gun blast parameters is attempted by least square fitting to obtain improved correlations. Otherwise, if a correlation is superior for one of the ideal scaling models, then only that model will be selected to improve correlation of the data with the use of the gun blast parameters.

4.1 Peak Overpressure Data Presented With Different Scaling Approaches

The data can first be examined along selected rays when the distance from the gun tube muzzle is scaled by ξ, corresponding to an explosion generated by a constant energy efflux. Figure 3 shows the peak overpressure data along the ray directed 30° from the muzzle axis.

When the data are scaled with the peak energy efflux approach, the slower emptying weapons (more resembling constant energy efflux) should have higher values of peak overpressure relative to the faster emptying weapons (less resembling constant energy efflux).

Least square fitting, discussed later in this section, will show that the weapons with the larger muzzle to Mach disc distances also tend to generate larger peak overpressures,

given equal values of δ_γ. The Mach disk location parameter is used because it was found to correlate data (Schmidt, Gion, & Fansler 1980), but a physical reason why this parameter could be used to improve correlation for either the constant energy efflux model or the point blast model is not known.

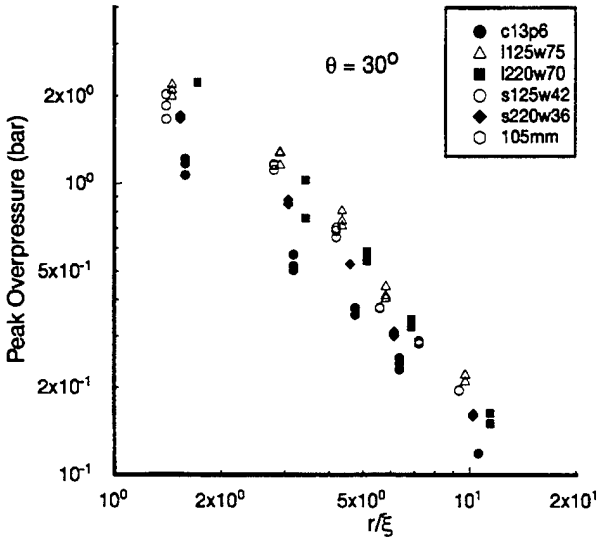

Figure 3. Scaled Peak Overpressure Data for $\theta = 30°$ (energy efflux assumption).

The results for Figure 3 indicate that the Mach disk position will correlate the data better than the blow-down parameter, when scaled for the constant energy efflux model. Nevertheless, the rapid blowdown for the 105-mm cannon appears to bring the data points into close company with other larger data values, even though the muzzle-to-Mach disk distance is larger than for any other firings. The c13p6 data have values for their parameters that would predict that the peak overpressure would be low compared to all the other data.

Figure 4 shows the peak overpressure data collected along the 90° angle to the bore axis. Again, the peak overpressure values obtained with the long barreled Magnum gun are higher than the values obtained with the short Magnum barrel (s125w42, s220w36), with the .30 caliber carbine (faster emptying but relatively small x_M/D) having the lowest peak overpressure. The 105-mm data again have higher average peak overpressures than the average with the highest value of x_M/D, yet with the lowest value of δ_ξ as shown in Table 2. The peak overpressure values for the ml0f250 data are lower than average and have the smallest value of x_M/D but have the highest value of δ_ξ.

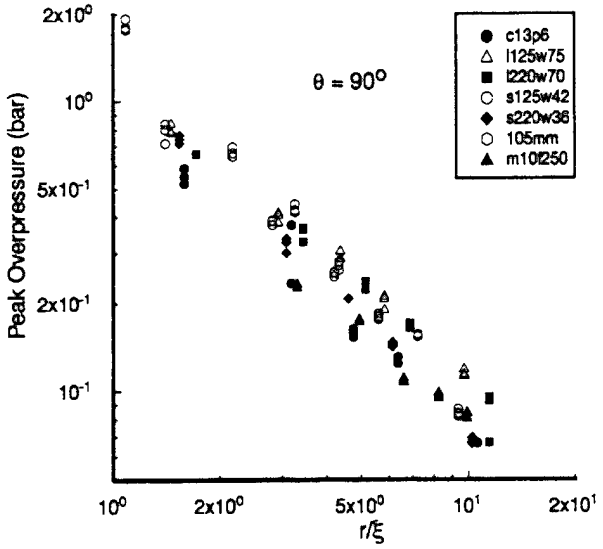

Figure 4. Scaled Peak Overpressure Data for $\theta = 90°$ (energy efflux assumption).

Figure 5 shows the peak overpressure data obtained along the ray at an angle of 150° to the bore axis direction. The peak overpressure data seem to be better correlated for 150° than for the data taken at the smaller polar angles.

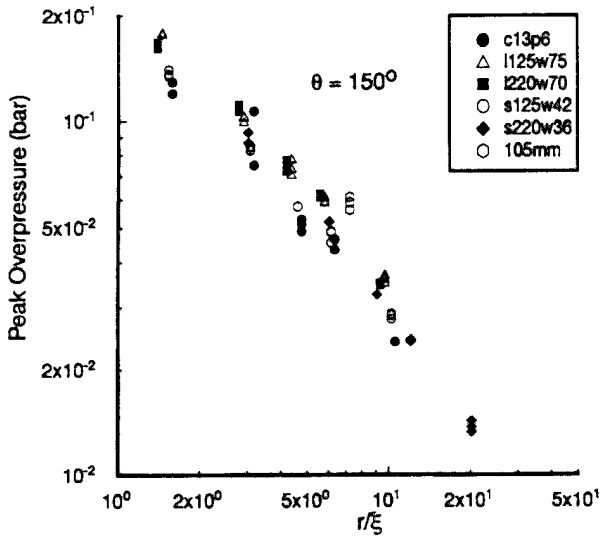

Figure 5. Scaled Peak Overpressure Data for $\theta = 150°$ (energy efflux assumption).

The peak overpressure data are next examined with the distance scaled by λ, corresponding to the point source explosion. Figure 6 shows the peak overpressure data along the 30° ray.

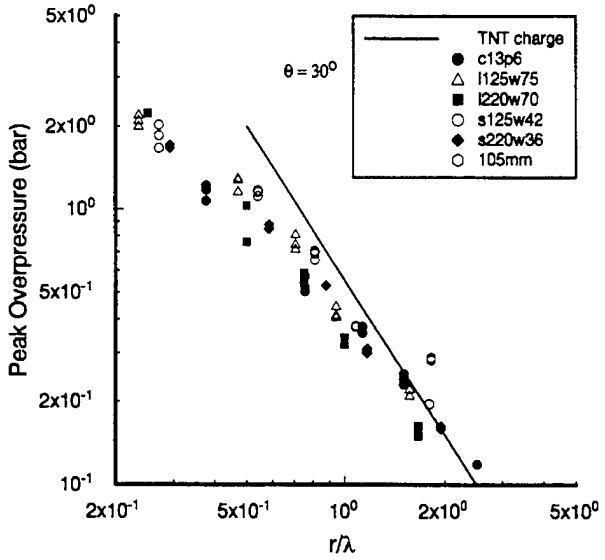

Figure 6. Scaled Peak Overpressure Data for θ = 30° (point source assumption) and Calculation for Trinitrotoluene (TNT) (Brode 1955, 1959) .

Also shown is a calculation for a spherical TNT charge in open air. The TNT calculations were obtained with a finite difference scheme developed by Brode (1955, 1959). The calculated values for the TNT charge should better approximate the ideal point source solution as the distance increase from the TNT charge. It is seen that the peak overpressure for the TNT charge is initially higher but decreases so rapidly that it is less than some of the gun blast data values at the longer scaled distances. Recall that smaller values of δ_λ are associated with a quicker emptying time (more resembling a point source) and should have higher peak overpressure values for a given distance, which generally occurs. The data show that the more rapidly emptying guns yield larger peak overpressures, as generally occurred when scaling was done with the point source scaling length. Some exceptions result from data scatter, the other reasons are not known. Figure 7 shows the peak overpressure along the 90° ray. The peak overpressure calculations obtained with a TNT charge could not be presented with Figure 7 because the peak overpressure data values are much lower than the calculation.

Again, the peak overpressures are higher for the guns that empty most rapidly, which agrees with physical intuition. The larger data spread in Figure 7 occurs because the 30-mm data (m10f250) are shown, which have the highest value of δ_λ.

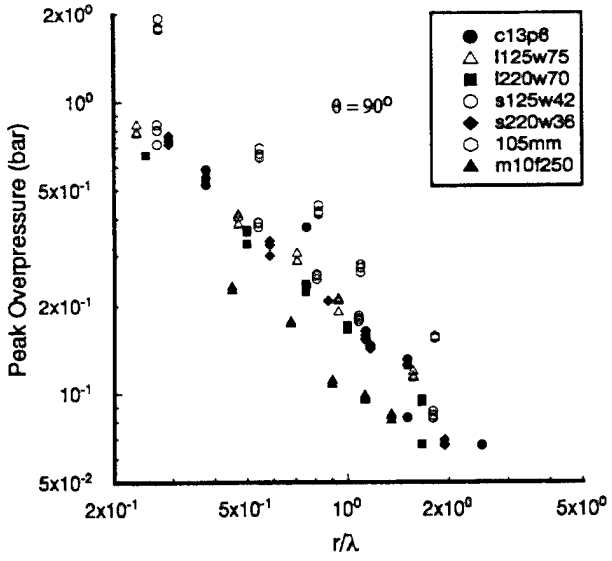

Figure 7. Scaled Peak Overpressure Data for θ = 90° (point source assumption).

The scaled peak overpressure values are shown in Figure 8 for θ = 150°. The trends are the same as for the prior two figures.

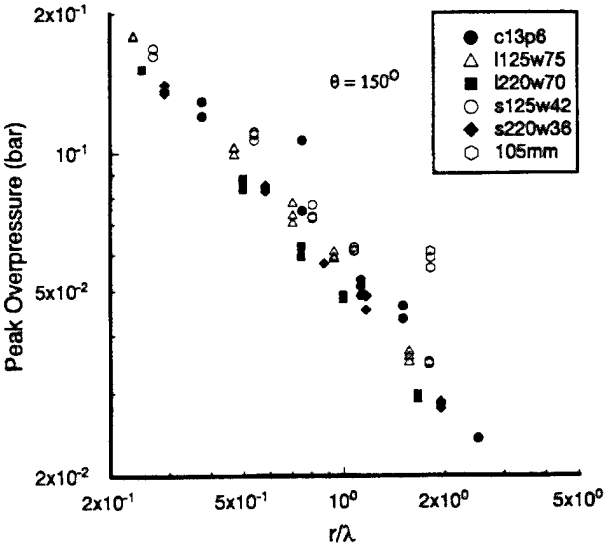

Figure 8. Scaled Peak Overpressure Data for θ = 150° (point source assumption).

Both unmodified approaches show deficiencies in correlating the data. It is not clear that either approach, when modified by the characteristic gun parameters, would be

noticeably superior to the other. Accordingly, least squares fitting are performed for both the point source model and the energy efflux model.

4.2 Modeling Approach for Peak Overpressure Data

The ideal scaling relationships, which assume spherically symmetrical conditions, need to be modified for gun blast, where the peak overpressure varies strongly with the polar angle, θ , from the boreline. Following Smith (1974), a directional scaling length factor is obtained, β, that depends on the polar angle,

$$\beta = \mu cos\theta + \sqrt{1 - \mu^2 sin^2\theta}\,, \tag{15}$$

in which μ is the momentum index, which determines the levels of peak overpressure (with distance held constant) as a function of the polar angle, θ. This expression has been developed from moving blast theory. The momentum of the charge results in the strength of the blast being increased in the direction of the momentum and decreased to the rear of the moving charge. The directional length scaling factor, β, is real and positive if $\mu < 1$. The nearer μ is to zero, the more nearly spherical the blast. As μ approaches 1, the strength of the blast in front of the gun becomes large compared to the strength of the blast wave to the rear.

To improve the prediction model, the scaling lengths, ξ and λ, need to be modified with the two gun blast parameters discussed earlier. Trial functions of these parameters are assumed as first order terms in a series expansion. Least square fitting showed that the most effective functions of these parameters involved the inverse of the blow-down parameter and the first power of the Mach disk location. Along with β to be determined by least squares fitting in terms of μ, two other constants that multiply these parameter functions need to be fitted to obtain the modified scaling lengths, ξ' and λ', defined by

$$\lambda' \equiv \lambda\beta\left(1 + \frac{C}{\delta_\lambda} + H\frac{x_M}{D}\right), \tag{16}$$

$$\xi' \equiv \xi\beta\left(1 + \frac{C}{\delta_\xi} + H\frac{x_M}{D}\right). \tag{17}$$

With these modifications, the gun blast peak overpressure is

$$\overline{P} = \overline{P}(\bar{r}) \tag{18}$$

in which $\bar{r} \equiv r / \ell$, and ℓ assumes the value of ξ' or λ', depending on the scaling approach used.

Also, the time of arrival, t_a, has its scaled equivalent,

$$\bar{t}_a\left(r/\ell\right) \equiv t_a a_\infty / \ell \tag{19}$$

The wave generated from gun blast decays to an acoustic wave

$$\left(\bar{P} \propto \left[\frac{1}{r}\right]\right)$$

at large distances, but closer in, the peak overpressure versus distance relationship has a steeper slope

$$\left(\bar{P} \propto \left[\frac{1}{r}\right]^a, a > 1\right),$$

as also occurs with instantaneous explosions. It is attempted to model this behavior with the following expression for the peak overpressure, $\bar{P}$,

$$\bar{P} = \frac{A}{\bar{r}} + \frac{B}{\bar{r}^2}. \tag{20}$$

Another more simple model will also be tried and compared with the two-term model:

$$\bar{P} = \frac{A}{\bar{r}^a}, \tag{21}$$

in which a is assumed to be constant throughout the region of interest. Equation (20) or Equation (21) is matched with pressure data in conjunction with Equation (15), which is the expression used to vary the strength of the blast with the polar angle, θ. The values of the significant parameters, λ/D, δ_λ, ξ/D, δ_ξ, and X_M/D, are given in Table 2. With these values and the peak overpressure data, fits are made to determine A, B, a, and μ for the one-term model, C, and H.

4.3 Peak Overpressure Fitting

Fits were made for both the point source model and the energy efflux model with the use of the blow-down parameters and Mach disc position. For the point source model, Table 3 gives the parameter values found for the predictive equations for both the one-term equation and the two-term equation.

The particular headings refer to the symbols occurring in Equations (15), (16), (17), (20), and (21). The one-term models (lpa, lpb, lpc, and lpd) are presented first in Table 3, in which $B = 0$ and $a \neq 1$. When C and H are assumed to be zero in the fitting procedure, the root mean square (RMS) error is 0.309. This value is obtained from fitting the logarithm of the pressure data with the logarithm of the fitting function. The RMS value of 0.309 translates to an expectation that the data value will be 36% more or less than the curve fit value. Fitting with the inverse blow-down parameter (model lpc) gives good improvement while fitting with Mach disc position (model lpb) yields significantly less improvement. Concurrent fitting with the blow-down and Mach disc position parameters gives only marginal improvement over fitting with the blow-down parameter. The two-term models (2pa and 2pb) give comparable results. The physical intuition that the scaled (point mass scaling) peak overpressures with longer blow-down times would be smaller relative to the peak overpressures for smaller blow-down times is confirmed by the positive fitted values for C.

Table 3. Least Squares Fit Results for Peak Overpressure Data (point source)

Model	μ	A	B	C	H	a	RMS
lpa	0.78	0.270	—	—	—	1.10	.309
lpb	0.78	0.145	—	—	.0374	1.09	.247
lpc	0.76	0.117	—	0.562	—	1.14	.199
lpd	0.77	0.100	—	0.564	.0159	1.13	.193
2pa	0.78	0.243	0.0220	—	—	—	.309
2pb	0.78	0.110	0.0061	0.592	—	—	.201

The results for the energy efflux model are presented in Table 4. The important parameter to improve fitting for the energy efflux model is the Mach disc position instead of the inverse blow-down parameter, $1/\delta\xi$, as it was for the point source model. The fit marginally improved with the use of the inverse blow-down parameter. The fit performed to fit values for both C and H (model led) gives a negative value for C and confirms the intuition that longer blow-down times result in higher scaled peak overpressures with the constant energy efflux model. The positive value obtained for C when H is assumed to be zero (1ec) occurs because there is a correlation between the blowdown and the Mach disk location parameter values. For a given gun configuration, increasing the charge mass results in a larger initial energy efflux and a smaller $\delta\xi$. The trend is noted in Table 2. When H is assumed to be zero (model 1ec), the effect of the Mach disk location overshadows the blow-down parameter and produces a false illusion.

For both the point source model and the energy efflux model, other fits were attempted with the gun parameters raised to other powers in Equations (16) and (17). These results are not shown as these particular choices yielded noticeably larger RMS errors than those shown.

Table 4. Least Squares Fit Results for Peak Overpressure Data (energy efflux model)

Model	μ	A	B	C	H	a	RMS
1ea	0.77	1.89	—	—	—	1.13	0.252
1eb	0.78	1.14	—	—	0.0248	1.10	0.208
1ec	0.77	1.77	—	0.107	—	1.12	0.251
1ed	0.77	1.18	—	-.349	0.0299	1.12	0.201
2ea	0.78	1.31	0.742	—	—	—	0.252
2eb	0.78	0.89	0.247	—	0.0271	—	0.210

The use of the blow-down parameter with the point source model significantly improves the data correlation while the use of the Mach disc position parameter with the constant energy efflux model markedly improves the data correlation. The point source model was selected as the basis for modification because, as will be seen in a later section, point source scaling correlates the impulse data better than the energy efflux scaling does. In terms of correlation, there is little to choose between the two-term modified point source model and the one-term modified point source model. The two-term modified point source model was selected in preference to the one-term model because the ratio of the peak overpressure to the front of the gun over the peak overpressure to the rear of the gun becomes larger nearer the gun muzzle, as experiment shows. Also, the expression for the time of arrival is simplified by the use of the two-term point source model with the blow-down parameter modification as compared with the use of the one-term expression. The selected fit to calculate future predicted fits for the peak overpressure is model 2pb in Table 3, which gives

$$\overline{P} = 0.11\frac{\lambda'}{r} + .0061\left(\frac{\lambda'}{r}\right)^2, \tag{22}$$

in which λ' is given by Equation (16), which varies with θ through β, as given by Equation (15). The scaled data with the prediction curve are shown in Figure 9. As expected, the carbine data (c13p6) show the most scatter, which may have to do with their gun blast parameter values. The parameters for the carbine are an unusual combination when compared with the other weapons. The carbine has the second smallest $\delta\lambda$ and the

second from the smallest muzzle-to-Mach disk distance in the group. If the other weapon's value of δ_λ were placed in increasing order, the value of x_M/D usually appears in declining order. Future studies should include weapons with similar characteristics to the carbine (c13p6).

Equation (22) gives good agreement over the parameter ranges where data were obtained. One should employ caution in extrapolating to parameter values outside the range where data were taken.

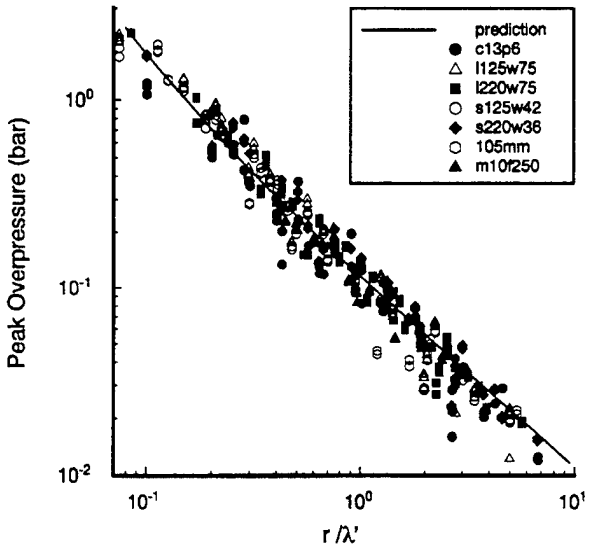

Figure 9. Peak Overpressure Versus r/λ With Least Squares Fit.

4.4 Modeling and Fitting Time-of-Arrival Data

As in Fansler and Schmidt (1983), the pressure-jump Mach relation,

$$\overline{P} = \frac{2\gamma}{\gamma+1}\left(\mathrm{M}_s^2 - 1\right), \tag{23}$$

can be equated to the predictive equation for peak overpressure, Equation (22). Here, M_S is the Mach number for the shock moving through still air. Because $dt_a/dr = 1/M_S$, the resulting expression can be integrated to obtain a closed form expression for the time of arrival, $\bar{t}_a$. The expression for the peak overpressure, Equation (20), when substituted into Equation (23) and integrated from the muzzle to the field point, r, becomes

$$\bar{t}_a - \bar{t}_o = X(\bar{r}) - \frac{A'}{2}\ln\left[2X(\bar{r}) + 2\bar{r} + A'\right], \tag{24}$$

in which

$$X(\bar{r}) = \sqrt{\bar{r}^2 + A'\bar{r} + B'}, \tag{25}$$

$$A' = \frac{2\gamma A}{\gamma + 1}, \qquad B' = \frac{2\gamma B}{\gamma + 1},$$

and $\lambda = 1.4$ is the specific heat ratio for ambient air. The initial time value, $\bar{t}_o$, takes into consideration the nature of the formation of the blast wave and may vary with the angle. The zero value for time corresponds to the projectile exiting the muzzle.

The time-of-arrival expression, Equation (24), can be used with the determined constants A, B, γ, and the time-of-arrival data to obtain the value, t_o, by a least squares fit

$$\bar{t}_a = X(\bar{r}) - 0.064\ln\left[2X(\bar{r}) + 2\bar{r} + 0.128\right] - 0.17, \tag{26}$$

in which

$$X(\bar{r}) = \sqrt{\bar{r}^2 + 0.128\bar{r} + 0.0074}.$$

Least squares fits were also tried to see if a directional dependence existed for the scaled time of arrival. The directional dependence was negligible.

Figure 10 shows the fitted curve for $\bar{t}_a$ as a function of the scaled length with the scaled time-of-arrival data.

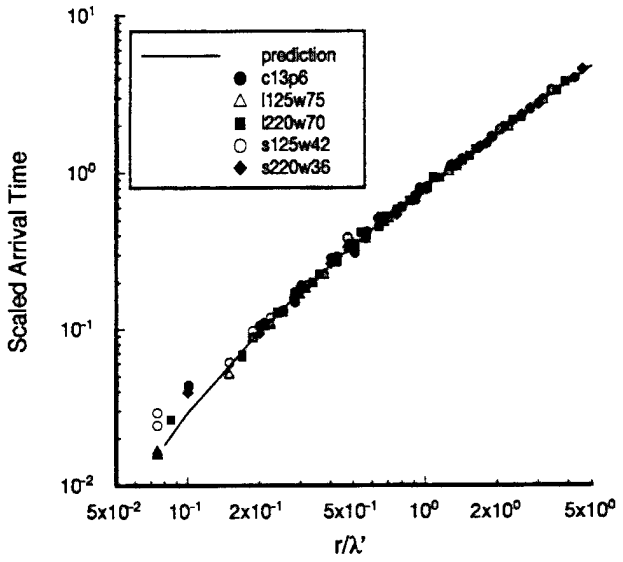

Figure 10. Predicted $\bar{t}_a$ Compared With the Observed $\bar{t}_a$.

A logarithmic scale was used to emphasize comparisons for the shorter scaled distances. The agreement of the data with the fitted time of arrival is satisfactory.

4.5 Impulse Data Presented With Different Scaling Approaches

Similarly, as for the peak overpressure data, the impulse data along selected direction rays (30°, 90°, and 150°) are scaled with both the ideal point source scale length and the energy efflux scale length. Figure 11 shows the impulse data obtained along a 30° ray when scaled using the constant energy efflux assumption.

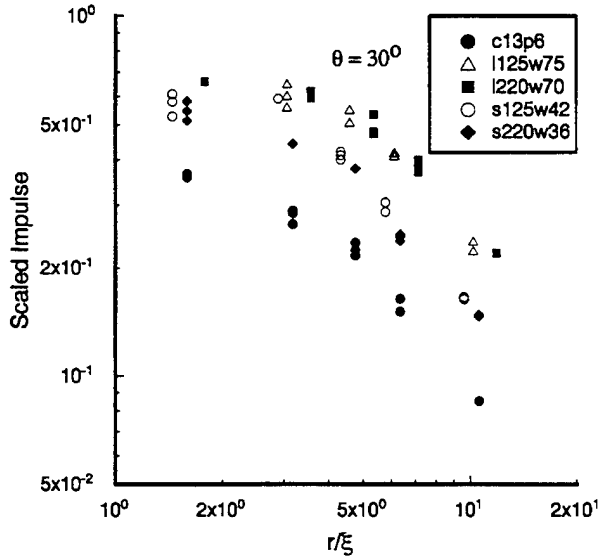

Figure 11. Scaled Impulse Versus r/ξ for θ = 30°.

The data do not appear to be well correlated using energy efflux scaling. The carbine (c13p6) empties rapidly and has the lowest impulse values while the long barreled Magnum with the largest projectile (1220w70) empties its barrel more slowly and is among the data with the higher values for the impulse. The impulse data for θ = 90° are shown in Figure 12. The same trends occur for Figure 12 with approximately the same spread.

The ml0f250 data for 90° are also shown, which have the highest value of $\delta\xi$, which correlates with higher peak overpressures and, most likely, with higher values for the scaled impulse. The ml0f250 data values are high but not the highest of the values shown in Figure 12. The Mach disk distance from the muzzle is also small compared with the distances for all the other gun configurations, which positively correlates with smaller

scaled values of peak overpressure and, one would think, smaller scaled values for the impulse. The impulse values for the ml0f250 data are a compromise between competing effects for two gun blast parameters. The scaled impulse values for the c13p6 firings are low compared with the rest of the data values, as also occurred for the measurements taken at θ = 30°. The gun-emptying time is small for the carbine and the distance from muzzle to Mach disk is not large compared to the results obtained with the other gun blast data.

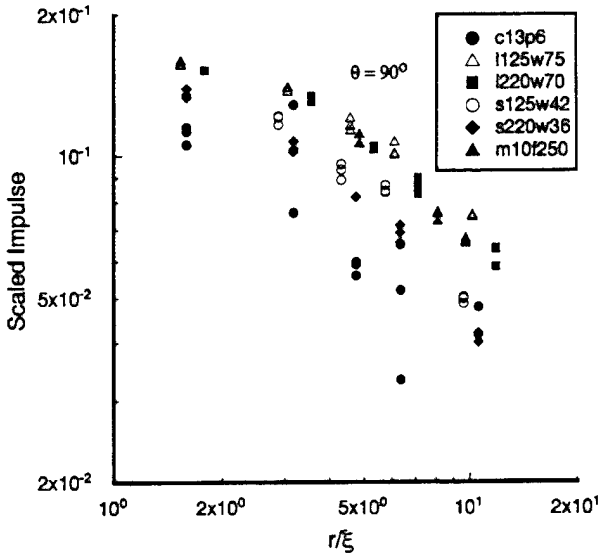

Figure 12. Scaled Impulse Versus r/ξ for θ = 90°.

Figure 13 shows the impulse data along the 150° ray. It is difficult to discern a trend here. As usual, the c13p6 data have the most scatter. Possibly, secondary flash-induced blast may be responsible for the larger amount of scatter at the largest polar angles.

In general, constant energy efflux scaling for the impulse data yields inferior correlations compared to the corresponding correlations for the peak overpressure data. This result seems physically reasonable because the peak value is more responsive to the early part of the energy efflux history while the shape of the wave would more strongly depend upon the complete energy efflux history.

Figure 14 shows the impulse data obtained along a 30° ray when point source scaled. Nearer the gun muzzle, the impulse decreases slowly at first and then descends much more rapidly for the longer distances. Apparently, energy flux flowing out of the gun continues to add to the blast as the wave passes over the first gauges used in this

investigation, and as the energy flux decreases, the curve steepens. The data are well correlated by point source scaling. The correlation is improved for the larger distances, which would be expected because almost all of the available energy would have been deposited by the time the front of the wave reaches the larger distances, while at the smaller distances, the various guns would have deposited different fractions of their total available energy. For the larger scaled distances, the correlation for the impulse at 30° is superior to the correlation obtained from the scaling investigation of the peak overpressure. The impulse is the time integral of the positive phase of the overpressure and would be expected to be a better indicator of the total energy deposited into generating the blast wave as compared to the peak overpressure. Nevertheless, the data points are, on the whole, slightly lower for the more slowly emptying guns, as occurs for the peak overpressure data.

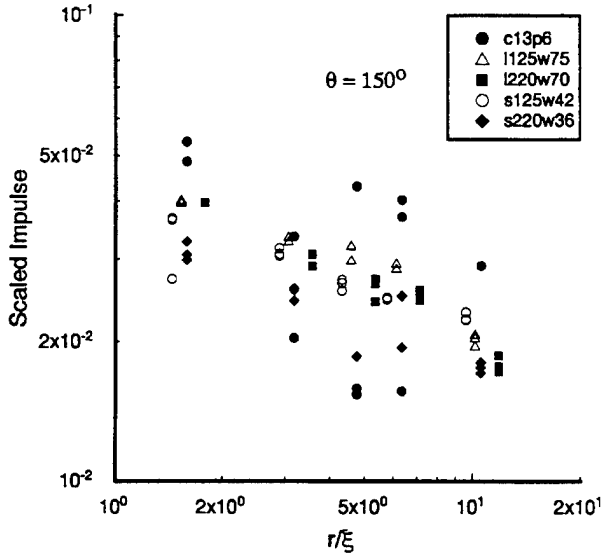

Figure 13. Scaled Impulse Versus r/ξ for θ = 150°.

The data for θ = 90° are shown in Figure 15. The ml0f250 data are also shown, which have the highest value of $\delta\lambda$. Overall, the curve descends more slowly than for Figure 14. Figure 16 shows the data along the 150° ray. The data descend yet more slowly than the data obtained at θ = 90°.

The impulse data values for point source scaling are better correlated than the impulse data values for constant energy efflux scaling. Accordingly, only the data that are point source scaled will be least squared fitted using the barrel-emptying parameter to improve the fit.

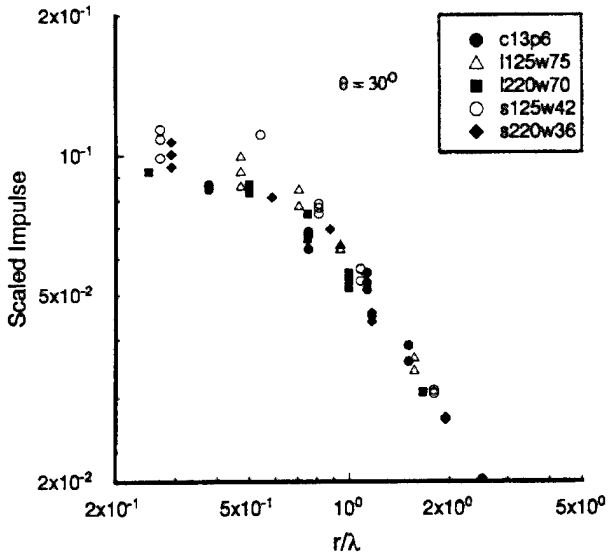

Figure 14. Scaled Impulse Versus r/λ for θ = 30°.

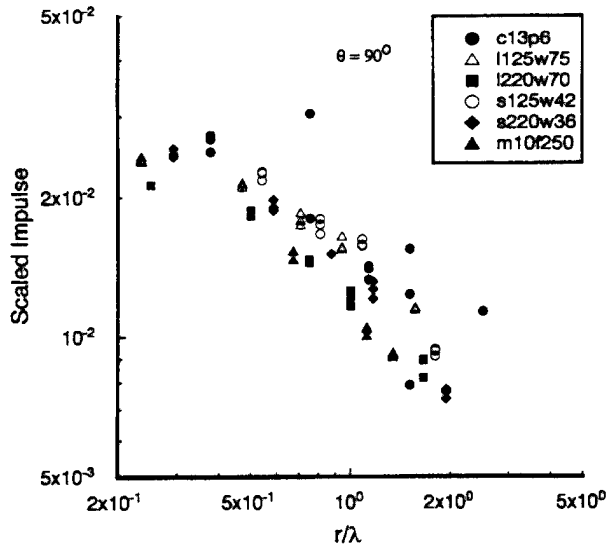

Figure 15. Scaled Impulse Versus r/λ for θ = 90°.

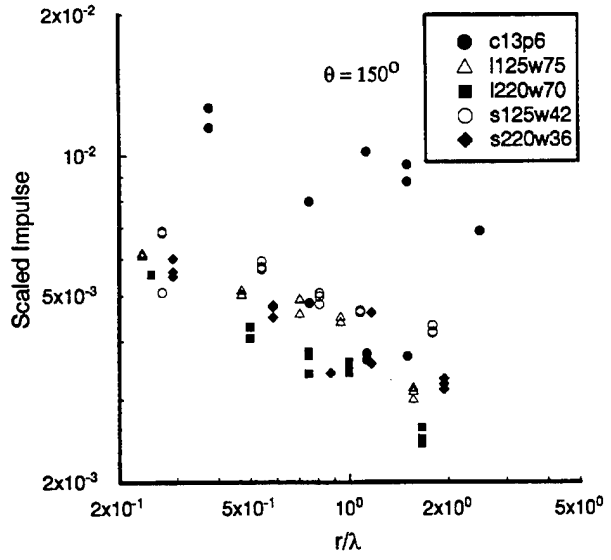

Figure 16. Scaled Impulse Versus r/λ for θ = 150°.

4.6 Modeling and Fitting Impulse Data

With the observations noted previously, candidate fitting equations may be proposed. The best candidate equation with its fitting coefficients are

$$\bar{I} = 0.0146\left(\frac{\lambda_i'}{r}\right)^{b_i(\theta)}, \tag{27}$$

in which

$$b_i(\theta) = 0.954 - 0.585\sin\frac{\theta}{2}, \tag{28}$$

and

$$\lambda_i' = \beta\left[1 + 0.444\frac{sin(\theta/2)}{\delta_\lambda}\right]\lambda \tag{29}$$

Note that the scaling length for the gun blast impulse differs from the scaling length for the peak overpressure, with the emptying parameter characterizing the gun blast, $\delta\lambda$, being applied more strongly to the rear of the gun. The least square fit was obtained using the logarithm of the impulse values as was done for the peak overpressure data. The RMS value was equal to 0.216, which is only a little larger than the RMS found for the peak overpressure data. Other more complicated fits were tried to account for the change in the slope with distance for the data forward of the gun, but only marginal

improvements in the RMS values were found. The dimensionless form of the impulse for gun blast is then

$$\bar{I} \equiv I a_\infty / \left(\lambda_1' p_\infty \right). \tag{30}$$

Unlike the presentation of the peak overpressure, when scaled with the modified point source length, the impulse data scaled by its special modified point source length must be presented with the polar angle as a parameter because $b_i(\theta)$ in Equation (27) varies with the polar angle. Figure 17 shows the impulse data scaled with the modified point source length for impulse together with the fitted curve for the 30° polar angle. The fitted curve is a compromise that, for small distances, is too high at first and then transitions to a region where it is too low and then becomes too large again.

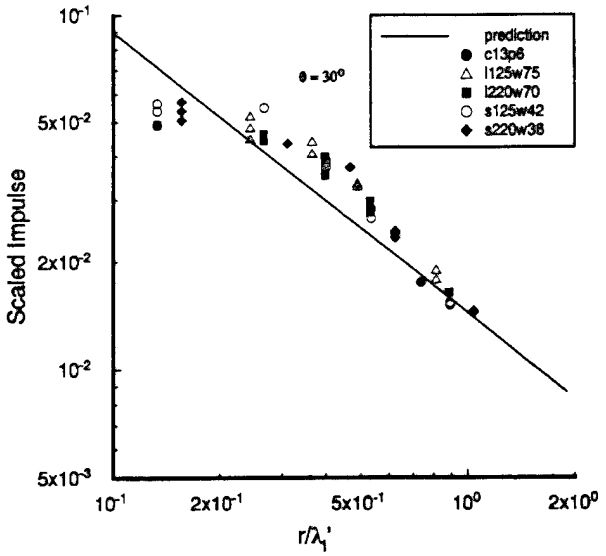

Figure 17. Scaled Impulse Versus r/λ_1' for $\theta = 30°$ With Least Squares Fit.

Figure 18 shows the scaled data with the fitted curve for 90°. Again, the fitted curve is but a straight line on the logarithmic graph, but the fitted curve now descends at a slower rate. Figure 19 shows the comparisons at 150°. The data are not correlated as well as they are for the smaller angles, and the c13p6 data have much shot-to-shot variability. The modified point source scaling approach successfully correlates the impulse data obtained to the front of the gun and can be used to gain physical insight into gun blast.

The flow processes are too complex to assume a form for the positive phase duration and to obtain an accurate estimate of its value from some simple assumptions. Moreover,

The flow processes are too complex to assume a form for the positive phase duration and to obtain an accurate estimate of its value from some simple assumptions. Moreover, accurate values of the positive-phase-duration data are more difficult to obtain because the overpressure varies slowly as the zero value of overpressure is approached, with smaller superimposed waves from turbulence in the flow resulting in large amounts of uncertainty for the time for the zero value of overpressure in the wave.

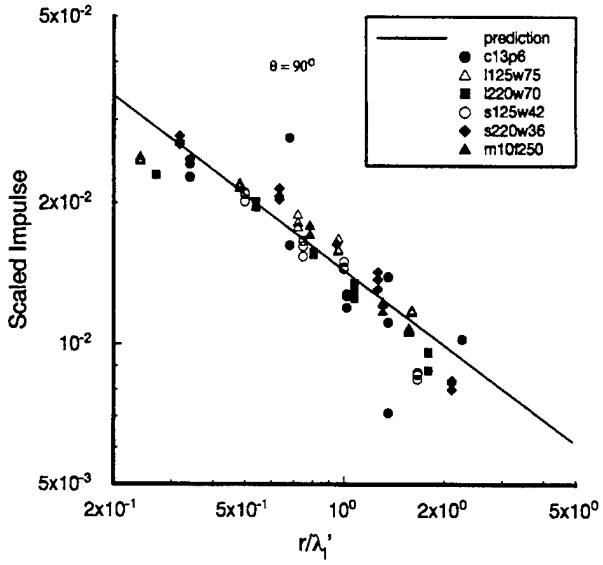

Figure 18. Scaled Impulse Versus r / λ_i' for $\theta = 90°$ With Least Squares Fit.

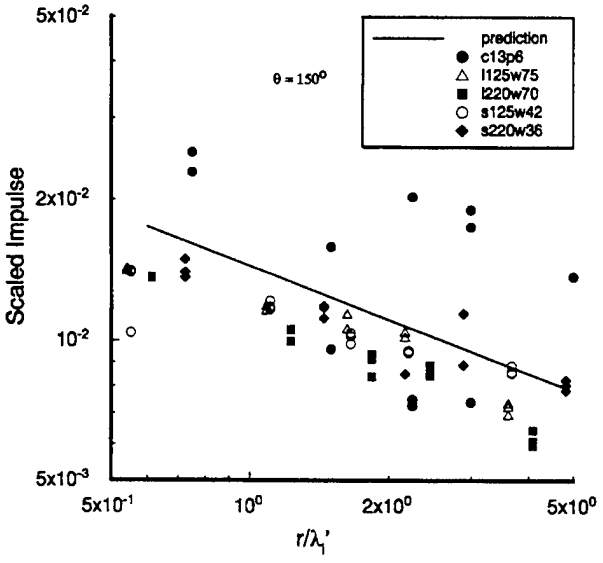

Figure 19. Scaled Impulse Versus r / λ_i' for $\theta = 150°$ With Least Squares Fit.

5. CONCLUSIONS AND RECOMMENDATIONS

Investigators have advocated particular approaches for describing gun muzzle blast. This investigation examines two principal approaches that use scaling ideal blast waves as a basic starting point. The data available consist of detailed overpressure records for weapons with a wide variety of locations, projectile weights, propellant weights, muzzle velocities, and barrel lengths. From the data, the peak overpressure, the time of arrival, and the impulse obtained by integrating the positive value of the overpressure wave with time are obtained.

The peak overpressure data are scaled using both the instantaneous energy release model and the constant energy deposition model. Neither of the scaling approaches gives a clearly superior correlation of the data. Two parameters that characterize gun blast are introduced for modification of the basic scaling approaches to improve data correlation. One is called the blow-down or emptying time parameter, while the other parameter gives the position of the Mach disc in terms of calibers. For the peak overpressure data scaled with the energy efflux length, the Mach disc position parameter noticeably improves correlation of the data, while the blow-down parameter value improves the correlation negligibly. For the data scaled with the point blast scaling length, the blow-down parameter is important for improving correlation, and the effect of the Mach disk location may be neglected. Slower emptying times result in an inefficient conversion of energy into the muzzle blast wave that reduces the peak overpressure. Both modified scaling approaches give similar improvements in correlation of the peak overpressure data. The modified point mass model was selected because the basic point mass model yielded a superior correlation for the impulse data. A two-term equation for predicting peak overpressure was selected that permits the development of a closed form expression describing the time of arrival and also approximates the nonlinear wave behavior near the muzzle.

The impulse data are also scaled with the two ideal models. The instantaneous energy release model correlates the data well to the front of the gun with less correlation as the polar angle is increased. The impulse decreases more slowly with distance as the polar angle increases. The constant energy deposition model does not correlate the impulse data as well as the point source model, particularly to the front of the gun. The point source model modified by the use of the gun-emptying parameter is used to develop a least squares fit function describing the data. The length scale developed for impulse data differs in form from the length scale for peak overpressure and depends upon the

polar angle, θ. Because of the angular dependence for the decay of the impulse value, the impulse data cannot be portrayed on a single graph. The RMS error obtained with the impulse data is only slightly larger than the error obtained for the peak overpressure data.

A prediction method for the positive phase duration is left for further investigations. More needs to also be known about the detailed flow processes in gun blast. Computational fluid dynamics techniques could be used to investigate the flow of energy from the front to the rear part of the wave and yield more insight into gun blast phenomena.

INTENTIONALLY LEFT BLANK

6. REFERENCES

Armendt, B. F., and J. Sperrazza. "Air Blast Measurements Around Moving Explosive Charges, Part III." BRL-MR-1019, U.S. Army Ballistic Laboratory, Aberdeen Proving Ground, MD, 1956.

Baker, W. E. "Explosions in Air." University of Texas Press, Austin, TX, 1973.

Brode, H. L. " ." Journal of Applied Physics, Vol. 26, p.766, 1955.

Brode, H. L. " ." Physics of Fluids, Vol. 2, p.217, 1959.

Corner, J. "Theory of the Interior Ballistics of Guns." John Wiley and Sons, Inc., New York, pp. 339-383, 1950.

Erdos, J. I., and P. DelGuidice. "Gas Dynamics of Muzzle Blast." AIAA Journal, Vol. 13, pp. 1048-1055, August 1975.

Fansler, K. S., and E. M. Schmidt. "The Prediction of Gun Muzzle Blast Properties Utilizing Scaling." ARBRL-TR-02504, U.S. Army Ballistic Research Laboratory, Aberdeen Proving Ground, MD, July 1983. (AD B07859)

Fansler, K. S. "Dependence of Free Field Impulse on the Decay Time of Energy Efflux for a Jet Flow." The Shock and Vibration Bulletin, Bulletin 56, Part 1, The Shock and Vibration Center, Naval Research Laboratory, Washington, DC, pp. 203-212, August 1986.

Fansler, K. S., W. P. Thompson, J. S. Carnahan, and B. J. Patton. "A Parametric Investigation of Muzzle Blast." ARL-TR-227, U.S. Army Ballistic Research Laboratory, Aberdeen Proving Ground, MD, September 1993.

Heaps, C. W., K. S. Fansler, and E. M. Schmidt. "Computer Implementation of a Muzzle Blast Prediction Technique." The Shock and Vi15ration Bulletin, Bulletin 56, Part 1, The Shock and Vibration Center, Naval Research Laboratory, pp. 213-230, August 1986.

Hopkinson, B. British Ordnance Minutes, 13565, 1915.

Kietzman, J., K. S. Fansler, and W. G. Thompson. "Muzzle Blast from 105mm M735 Round." ARBRL-MR-3957, U.S. Army Ballistic Research Laboratory, Aberdeen Proving Ground, MD, January 1992. (AD A245565)

Pater, L. L. "Gun Blast Far Field Peak Overpressure Contours." TR 79-442, Naval Surface Weapons Center, Dahlgren, VA, March 1981.

Reynolds, B. T. "Muzzle Blast Pressure Measurements." Report No. PMR-21, Princeton University, April 15, 1944.

Schmidt, E. M., E. J. Gion, and K. S. Fansler. "Analysis of Weapon Parameters Controlling the Muzzle Blast Overpressure Field." Fifth International Symposium on Ballistics, Toulouse, Fance, April 1980.

Smith, F. "A Theoretical Model of the Blast from Stationary and Moving Guns." First International Symposium on Ballistics, Orlando, FL, 13-15 November 1974.

Soo Hoo, G., and G. R. Moore. "Scaling of Naval Gun Blast Peak Overpressures." TN-T7-72, Naval Surface Weapons Center, Dahlgren, VA, August 1972.

Westine, P. "The Blast Field about the Muzzle of Guns." Shock and Vibration Bulletin, Vol 39, pp. 139-149, March 1969.

NO. OF COPIES	ORGANIZATION
2	ADMINISTRATOR DEFENSE TECHNICAL INFO CENTER ATTN DTIC DDA 8725 JOHN J KINGMAN RD STE 0944 FT BELVOIR VA 22060-6218
1	DIRECTOR US ARMY RESEARCH LABORATORY ATTN AMSRL CS AL TA/RECORDS MGMT 2800 POWDER MILL ROAD ADELPHI MD 20783-1197
1	DIRECTOR US ARMY RESEARCH LABORATORY ATTN AMSRL CI LL/TECH LIB 2800 POWDER MILL ROAD ADELPHI MD 20783-1197
1	DIRECTOR US ARMY RESEARCH LABORATORY ATTN AMSRL CS AL TP/TECH PUB 2800 POWDER MILL ROAD ADELPHI MD 20783-1197
1	COMMANDER U S ARMY ARMAMENT MUNITIONS AND CHEMICAL COMMAND ATTN AMSMC LEP L ROCK ISLAND IL 61299-5000
1	DIRECTOR U S ARMY MISSILE & SPACE INTELLIGENCE CENTER ATTN AIAMS YDL REDSTONE ARSENAL AL 35898-5000
1	COMMANDER US ARMY ARMAMENT RD&E CENTER ATTN AMSTA AR TD MR HIRSHMAN PICATINNY ARSENAL NJ 07806-5000
6	COMMANDER US ARMY ARMAMENT RD&E CENTER ATTN AMSTA AR AET A MR S KAHN MR M AMORUSO MR PEDERSEN MR C NG MR W TOLEDO MR B WONG PICATINNY ARSENAL NJ 07801-5000
1	COMMANDER US ARMY ARMAMENT RD&E CENTER ATTN AMSTA AR CCL D S LISS PICATINNY ARSENAL NJ 07801-5000

NO. OF COPIES	ORGANIZATION
2	COMMANDER U S ARMY TANK AUTOMOTIVE CMD ATTN AMCPM BFVS AMCPM BFVS SC K PITCO WARREN MI 48397-5000
1	COMMANDER U S ARMY MISSILE COMMAND ATTN AMSMI RD DR W WALKER REDSTONE ARSENAL AL 35898-5000
1	COMMANDER TANK MAIN ARMAMENT SYSTEMS ATTN AMCPM TMA R BILLINGTON PICATINNY ARSENAL NJ 07806-5000
2	COMMANDANT U S ARMY INFANTRY SCHOOL ATTN ATSH IV SD R GORDAY ATSH TSM FORT BENNING GA 31905-5660
3	DIRECTOR BENET LABORATORIES ATTN SMCAR CCB J BENDICK SMCAR CCB DS P VOTTIS SMCAR CCB RA WATERVLIET NY 12189-4050
1	COMMANDER ARMY RESEARCH OFFICE ATTN AMXRO MCS MR K CLARK P O BOX 12211 RESEARCH TRIANGLE PARK NC 27709-2211
1	COMMANDER ARMY RESEARCH OFFICE ATTN AMXRO RT IP LIBRARY SVS P O BOX 12211 RESEARCH TRIANGLE PARK NC 27709-2211
1	COMMANDER AVIATION APPLIED TECHNICAL DIR ATTN SAVRT TY MSMA G MOFFATT PICATINNY ARSENAL NJ 07801-5000 FORT EUSTIS VA 23604-5577

NO. OF COPIES	ORGANIZATION
3	DEPARTMENT OF THE ARMY CONSTRUCTION ENGINEERING RESEARCH LABORATORY ATTN CERL SOI P SCHOMER L PATER J WILCOSKI P O BOX 4000 CHAMPAIGN IL 61820
2	COMMANDER ASD/YHT ATTN WL/MNAA CPT J PALUMBO ASD/YHT D CURLEY EGLIN AFB FL 32542
1	COMMANDER (CODE 3433) NAVAL WARFARE CENTER ATTN TECH LIB CHINA LAKE CA 93555
2	COMMANDER NAVAL SURFACE WARFARE CENTER ATTN 6X J YAGLA G MOORE DAHLGREN VA 22448
1	COMMANDER (CODE 6120C) NAVAL ORDNANCE STATION ATTN SUSAN PETERS INDIAN HEAD MD 20640
1	COMMANDER (CODE 3892) NAVAL WARFARE CENTER ATTN K SCHADOW CHINA LAKE CA 93555
1	COMMANDER (CODE 730) NAVAL SURFACE WARFARE CENTER SILVER SPRING MD 20910
1	DIRECTOR NASA SCIENTIFIC & TECHNICAL INFORMATION FACILITY ATTN SAK/DL PO BOX 8757 BALTIMORE/WASHINGTON INTERNATL AIRPORT MD 21240
1	MCDONNELL DOUGLAS ATTN JOSEPH SMUCKLER 1014 FERNGATE LANE CREVE COEUR MO 63141

NO. OF COPIES	ORGANIZATION
1	HONEYWELL COMPANY ATTN J GLASER S LANGLEY UNITED DEFENSE ARMAMENTS SYSTEM DIV 4800 EAST RIVER ROAD MINNEAPOLIS MN 55343
1	S & D DYNAMICS INC ATTN R BECKER 7208 MONTRICO DR BOCA RATON FL 33433
1	AAI CORPORATION ATTN T STASNEY P O BOX 126 MS 100-405 HUNT VALLEY MD 21030-0126
2	AEROJET GENERAL CORPORATION ATTN W WOLTERMAN A FLATAU P O BOX 296 AZUSA CA 91702
2	LOCKHEED AIRCRAFT INC ATTN J BROWN J PEREZ PO BOX 33 DEPT 1-330/UPLAND ONTARIO CA 91761
1	GENERAL ELECTRIC ARMAMENT & ELECTRIC SYSTEMS ATTN R WHYTE LAKESIDE AVENUE BURLINGTON VT 05401
1	FRANKLIN INSTITUTE ATTN TECH LIBRARY RACE & 20TH STREETS PHILADELPHIA PA 19103
1	THE JOHNS HOPKINS UNIV/CPIA 10630 LITTLE PATUXENT PARKWAY SUITE 202 COLUMBIA MD 21044-3200
2	LORAL CORPORATION ATTN S SCHMOTOLOCHA B AXELY 300 N HALSTEAD ST PO BOX 7101 PASADENA CA 91109

NO. OF COPIES	ORGANIZATION
2	MCDONNELL-DOUGLAS HELICOPTER CO ATTN D VAN OSTEEN R WATERFIELD MAIL STATION D216 500 E MCDOWELL RD MESA AZ 85205
1	FN MANUFACTURING INC ATTN GEORGE KONTIS POST OFFICE BOX 24257 COLUMBIA SC 29224
2	ARROW TECH ASSOCIATES INC ATTN ROBERT WHYTE WAYNE HATHAWAY 1233 SHELBURNE ROAD SUITE D8 SOUTH BURLINGTON VT 05403
1	GEORGIA INST OF TECHNOLOGY THE GEORGE W WOODRUFF SCHOOL OF MEHANICAL ENGINEERING ATTN DR G P NEITZEL ATLANTA GA 30332
1	UNITED DEFENSE LP ATTN SUZANNE DAVISON ARMAMENT SYSTEMS DIVISION 4800 EAST RIVER RD (MAIL STOP M239) MINNEAPOLIS MN 55421
1	OLD DOMINION UNIVERSITY MATHEMATICS DEPARTMENT ATTN DR CHARLIE COOKE NORFOLK VA 23508
1	SCITEC INC ATTN ALEX ZISLAN 100 WALL STREET PRINCETON NJ 08540
1	LOS ALAMOS NATIONAL LAB ATTN THOMAS DAVIS GROUP WX 4 MS G787 LOS ALAMOS NM 87545
1	OLIN CORPORATION ATTN STEPHAN FAINTICH PO BOX 222 ST MARKS FL 32355
1	ATLANTIC RESEARCH CORP ATTN MARK FRIEDLANDER 5945 WELLINGTON ROAD MS G787 GAINESVILLE VA 22065
2	UNIVERSITY OF VIRGINIA DEPT OF MECH AND AEROSPACE ENGINEERING ATTN H G WOOD III J MORTON CHARLOTTESVILLE VA 22901
	ABERDEEN PROVING GROUND
2	DIRECTOR US ARMY RESEARCH LABORATORY ATTN AMSRL CI LP (TECH LIB) BLDG 305 APG AA
2	DIR USAMSAA ATTN AMXSY D W BROOKS R CONROY
5	CDR USAATC ATTN STECS AAL M MAULE STECS AS LA S WALTON STECS DA P PAULES STECS AS HP J ANDREWS BLDG 400
2	CDR USATECOM ATTN AMSTE TE R MR KEELE AMSTE TA R W MARSHALL RYAN BLDG
1	DIR AMC INT MAT EVAL DIV ATTN AMCICP IM R BLOOM
4	DIR USAARDEC ATTN SMCAR FSF T R LIESKE J MATTS R PUHALLA J WHITESIDE FIRING TABLES BRANCH BLDG 120
40	DIR USARL ATTN AMSRL WM I MAY AMSRL WM P A HORST E SCHMIDT AMSRL WM PA T MINOR G KELLER M NUSCA AMSRL WM PC R FIFER

NO. OF COPIES	ORGANIZATION
	AMSRL WM PD B BURNS
	AMSRL WM W C MURPHY
	AMSRL WM WB W D'AMICO
	B DAVIS
	F BRANDON
	G BROWN
	AMSRL WM WC J BORNSTEIN
	R VON WAHLDE
	AMSRL WT PB K FANSLER (5)
	P PLOSTINS
	D WEBB
	G COOPER (2)
	M BUNDY
	B PATTON
	K SOENCKSEN
	V OSKAY
	J GARNER
	P WEINACHT
	B GUIDOS
	H EDGE
	J SAHU
	A MIKHAIL
	A ZIELINSKI
	AMSRL HR SD J KALB
	AMSRL SC C C NIETUBICZ
	AMSRL SC CC A CELMINS

REPORT DOCUMENTATION PAGE

Form Approved
OMB No. 0704-0188

1. AGENCY USE ONLY *(Leave blank)*	2. REPORT DATE	3. REPORT TYPE AND DATES COVERED
	September 1997	Final

4. TITLE AND SUBTITLE

Description of Gun Muzzle Blast by Modified Ideal Scaling Models

5. FUNDING NUMBERS

PR: 1L162618AH80

6. AUTHOR(S)

Fansler, K. S. (ARL)

7. PERFORMING ORGANIZATION NAME(S) AND ADDRESS(ES)

U.S. Army Research Laboratory
Weapons & Materials Research Directorate
Aberdeen Proving Ground, MD 21010-5066

8. PERFORMING ORGANIZATION REPORT NUMBER

9. SPONSORING/MONITORING AGENCY NAME(S) AND ADDRESS(ES)

U.S. Army Research Laboratory
Weapons & Materials Research Directorate
Aberdeen Proving Ground, MD 21010-5066

10. SPONSORING/MONITORING AGENCY REPORT NUMBER

ARL-TR-1434

11. SUPPLEMENTARY NOTES

12a. DISTRIBUTION/AVAILABILITY STATEMENT

Approved for public release; distribution is unlimited.

12b. DISTRIBUTION CODE

13. ABSTRACT *(Maximum 200 words)*

Gun blast data from a large variety of weapons are scaled and presented for both the instantaneous energy release and the constant energy deposition rate models. For both ideal explosion models, similar amounts of data scatter occur for the peak overpressure but the instantaneous energy release model correlated the impulse data significantly better, particularly for the region in front of the gun. Two parameters that characterize gun blast are used in conjunction with the ideal scaling models to improve the data correlation. The gun-emptying parameter works particularly well with the instantaneous energy release model to improve data correlation. In particular, the impulse, especially in the forward direction of the gun, is correlated significantly better using the instantaneous energy release model coupled with the use of the gun-emptying parameter. The use of the Mach disk location parameter improves the correlation only marginally. A predictive model is obtained from the modified point source correlation.

14. SUBJECT TERMS

impulse noise
muzzle blast
noise management
overpressure

15. NUMBER OF PAGES
48

16. PRICE CODE

17. SECURITY CLASSIFICATION OF REPORT	18. SECURITY CLASSIFICATION OF THIS PAGE	19. SECURITY CLASSIFICATION OF ABSTRACT	20. LIMITATION OF ABSTRACT
Unclassified	Unclassified	Unclassified	

NSN 7540-01-280-5500

Standard Form 298 (Rev. 2-89)
Prescribed by ANSI Std. Z39-18
298-102